Incremental Nonlinear Dynamic Inversion Control of Long-Stroke Pneumatic Actuators

Das, H.; Pool, D.M.; van Kampen, E.

Publication date
2021

Document Version
Accepted author manuscript

Published in
European Control Conference

Incremental Nonlinear Dynamic Inversion Control of Long-Stroke Pneumatic Actuators

Hemjyoti Das[1], Daan Pool[2] and Erik-Jan van Kampen[3]

***Abstract*— Pneumatic cylinders provide an environment-friendly actuation means by minimizing the leakage of any harmful industrial fluids, as occurs for hydraulic actuators. However, pneumatic actuation has not been utilized widely for industrial servo applications due to its highly nonlinear nature. Incremental nonlinear dynamic inversion (INDI) is a form of nonlinear dynamic inversion (NDI) that relies less on plant-model information, and is thus inherently robust to mismatches in the known plant-model, and also to external disturbances. Developing an incremental nonlinear controller for a pneumatic system is the main focus of this research article, which is accomplished by utilizing a cascaded-control approach, where the inner-loop INDI tracks a given force and the outer-loop NDI is for controlling the piston-position. Moreover, realistic sensor noises have been added in the simulation and the robustness of the incremental approach is demonstrated with respect to a baseline PID controller.**

I. INTRODUCTION

One of the common means of actuation for controlling a machine is pneumatic actuation. The working medium of a pneumatic cylinder is compressed-air [1], whereas hydraulic cylinders use a mineral oil based-fluid [2]. These hydraulic fluids can leak into the environment and can become a major source of pollution [3]. This external-leakage might further lead to internal-leakage and also wearing of the cylinder components [4]. These shortcoming of a hydraulic actuator can be overcome by replacing it with a safer pneumatic actuation. Thus, pneumatic actuators require less maintenance, compared to hydraulics and can be economically beneficial for a number of industries.

Pole-placement is one of the first developed controllers for a pneumatic actuator [5], but the limitations of its dynamic model and hardware forced the feedback-gains to be high. Various adaptive control methods have also been explored to estimate the unknown model parameters [6], [7], in order to get a better control performance. Techniques of back-stepping [8] and sliding mode [9] controller have also been applied for the control of pneumatic actuators. A comparative-study of some of these nonlinear controllers shows improvement over the conventional linear control techniques. However, in some cases, model-based adaptive control techniques demand an iterative process to identify the accurate model of a system, which further requires immense validation and verification [10].

Recent developments in incremental nonlinear dynamic inversion (INDI) control have led to its widespread use for aerospace control applications [11], [12]. INDI combines the advantages of an incremental form with that of a model-based nonlinear dynamic inversion (NDI) [13] to result in a robust controller that relies less on the system model and depends more on the accuracy of sensor feedback [12]. Currently, there is no available research work that exploited INDI control for pneumatic actuation, which is the main focus of this paper.

A number of industrial pneumatic actuators are currently being controlled by conventional PID controllers [14], [1], mainly due to its ease of implementation. However, the performance of linear controllers for a nonlinear system is likely to degrade under varying operating conditions [5]. Therefore, a conventional PID controller has been implemented here as a baseline controller and the second contribution of this research article is to highlight the advantages of incremental-control over a conventional linear-control strategy, in the context of a pneumatic system. Realistic sensor noises are introduced and the external load attached to the piston is varied in order to compare the robustness property between PID and the incremental approach.

II. PNEUMATIC SYSTEM DYNAMICS

A schematic diagram of a pneumatic system is shown in Fig. 1 [15]. The dynamics of piston and the connected

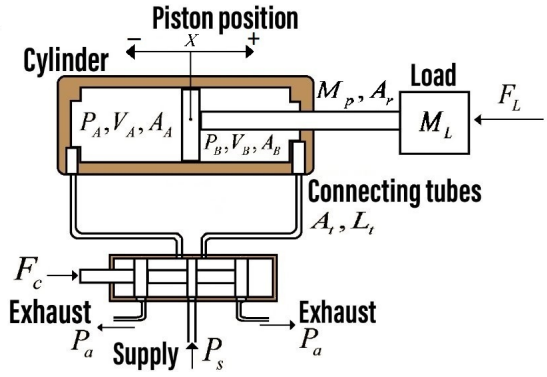

Fig. 1: Schematic diagram of a pneumatic system

external-load can be described by the following equation:

$$(M_L + M_p)\,\ddot{x} + F_f + F_L = P_A A_A - P_B A_B - P_a A_r \quad (1)$$

[1]Hemjyoti Das is with the Faculty of Aerospace Engineering, Delft University of Technology; Kluyverweg 1, 2629HS, Delft, The Netherlands. hemjyoti.nit@gmail.com

[2]Daan Pool is with the Faculty of Aerospace Engineering, Delft University of Technology; Kluyverweg 1, 2629HS, Delft, The Netherlands. d.m.pool@tudelft.nl

[3]Erik-Jan van Kampen is with the Faculty of Aerospace Engineering, Delft University of Technology; Kluyverweg 1, 2629HS, Delft, The Netherlands. E.vanKampen@tudelft.nl

In Eq. (1), x is the position of the piston, P_A and P_B are the pressures in chambers A and B, respectively, whereas A_A and A_B are the respective areas of chamber A and B. P_a denotes the ambient atmospheric-pressure. M_L refers to the mass of the external-load and M_p denotes the mass of cylinder-piston including the rod. F_L refers to the force due to the external load and A_r is the cross-sectional area of the piston rod. A Coulomb friction-force acts between the piston and the inner-surface of cylinder, which is represented by F_f.

Next, the rate of change of pressure across each cylinder-chamber is represented as follows [15]:

$$\dot{P}_i = \frac{RTk}{V_i}\left(\alpha_{in}\dot{m}_{\mathrm{in,i}} - \alpha_{out}\dot{m}_{\mathrm{out,i}}\right) - \frac{P_i k}{V_i}\dot{V}_i \tag{2}$$

In Eq. (2), the subscript i can be either A or B, depending on the chamber. R is the non-dimensional ideal gas constant and the temperature T is considered as the room-temperature. $\dot{m}_{\mathrm{in,i}}$ and $\dot{m}_{\mathrm{out,i}}$ respectively refers to the rate of mass-inflow and mass-outflow from the cylinder chamber i. α_{in} and α_{out} are the thermal coefficients that are characteristics of the compression and expansion process, respectively. k is the specific heat ratio of the atmospheric air and V_i refers to the volume of cylinder chamber i that can be expressed using Eq. (3).

$$V_i = V_{0i} + A_i\left(\frac{1}{2}L \pm x\right) \tag{3}$$

In Eq. (3), V_{oi} and A_i refers to the inactive-volume and area of chamber i, respectively. V_{oi} is equal to the product of chamber area A_i and the equivalent length of dead volume denoted as L_0 in Table. I. L refers to the total length of one-complete piston stroke.

The mass-flow rate from a pneumatic valve to the cylinder can be either classified as chocked or unchoked, depending on the ratio of down-stream to up-stream chamber-pressure [15], as summmarized in Eq. (4).

$$\dot{m}_v = \begin{cases} C_f A_v C_1 \frac{P_u}{\sqrt{T}} & \text{if } \frac{P_d}{P_u} \leqslant P_{cr} \\ C_f A_v C_2 \frac{P_u}{\sqrt{T}}\left(\frac{P_d}{P_u}\right)^{1/k}\sqrt{1-\left(\frac{P_d}{P_u}\right)^{(k-1)/k}} & \text{if } \frac{P_d}{P_u} > P_{cr} \end{cases} \tag{4}$$

In Eq. (4), C_f, C_1 and C_2 are the nondimensional discharge constants whereas P_u and P_d denotes the upstream and downstream pressure, respectively. P_{cr} is the critical pressure, which depends on the specific heat ratio. Finally, A_v represents the orifice opening, which controls the flow of air through a pneumatic-valve. The pneumatic valve is modelled as first-order dynamics between the commanded orifice-opening (A_v) from the controller and the actual orifice-opening (A_{v_m}) that is supplied to the plant.

III. Incremental Nonlinear Dynamic Inversion Control (INDI)

Incremental Nonlinear Dynamic Inversion (INDI) is a recently developed control-technique, which has been used widely for aerospace applications [11]. It is more robust compared to NDI [16] in handling external disturbances and system uncertainties, due to its marginal dependency on the plant dynamics. The basic principle of INDI is that it combines the advantages of model inversion with that of incremental approach to result in a control-command that relies mores on the accuracy of the sensor feedback and depends less on the system-dynamics. In order to frame an INDI control, a general nonlinear plant is defined as $\dot{\mathbf{x}} = \mathbf{f}(\mathbf{x}, \mathbf{u})$, where $\mathbf{x}$ and $\mathbf{u}$ refers to the state vector and the supplied control-input, respectively. Taylor-series expansion can be used to expand $\mathbf{f}(\mathbf{x}, \mathbf{u})$ and then the higher-order terms are neglected to obtain an simplified expression [11]. Next, considering a high sampling-rate and using time-scale separation principle, it is assumed that the update-rate of the control-command $\mathbf{u}$ is much higher than that of the state $\mathbf{x}$. Therefore, the state-Jacobian term is dropped [11]. Finally by using inversion and by introducing the linear enforcement-dynamics $\ddot{\mathbf{x}} = \mathbf{v}$, the total control-command generated from INDI is summarized in Eq. (5).

$$\mathbf{u} = \mathbf{u}_0 + \mathbf{G}\left(\mathbf{x}_0, \mathbf{u}_0\right)^{-1}\left(\mathbf{v} - \dot{\mathbf{x}}_0\right) \tag{5}$$

In Eq. (5), $\mathbf{x_0}$ and $\mathbf{u_0}$ refers to the system-state and control-command at the previous time-instant, respectively. The chosen linear-law $\mathbf{v}$ will guarantee an asymptotic stability of the plant-output error, and it will be discussed in more details in Section IV. It can be observed from Eq. (5) that the final expression of control-command does not contain any information of the state-transition matrix [11], and is thus less-dependent on the system dynamics. However, it is dependent on the feedback of the state-derivative, and thus an erroneous feedback of $\dot{\mathbf{x}}_0$ can reduce the efficiency of INDI. In Eq. (5), the matrix $\mathbf{G}(\mathbf{x_0}, \mathbf{u_0})$ denotes the jacobian of the plant model $\mathbf{f}(\mathbf{x}, \mathbf{u})$ with respect to the control command $\mathbf{u}$ at the operating points $\mathbf{x}_0$ and $\mathbf{u}_0$. $\mathbf{G}(x_0, u_0)$ should be invertible and thus should be a full-rank matrix. For our case, it is a 1×1 non-zero matrix and is thus always full-rank. It is also proved that if the considered system has a high sampling-rate, then the uncertainties in control-effectiveness does not influence the performance of the incremental control approach INDI. The stability and robustness analysis of INDI can be found in more details in [17].

IV. Controller Design for a Pneumatic System

A cascaded strategy of pneumatic control is discussed in this section. It is similar in principle to that of a cascaded hydraulic controller [18], which is summarized in Fig. 2.

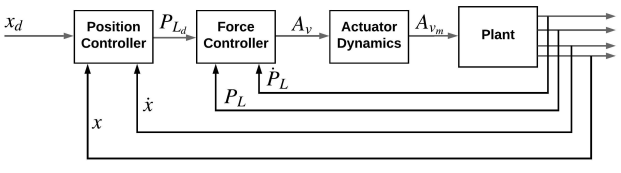

Fig. 2: Block diagram of an cascaded control approach

The outer-loop is known as the position control loop, which is fed with the desired piston-position x_d. It also receives the feedback of the actual piston-position x and

its velocity $\dot{x}$. Based on their error, the desired pressure-difference P_{L_d} across the two chambers is calculated, which is then fed to the inner-loop force controller. The inner-loop receives the feedback of the actual pressure-difference P_L across the two chambers, and also its time-derivative $\dot{P}_L$. The output of the inner-loop controller is the commanded orifice-opening A_v of pneumatic valve, which is then acted upon by a first-order valve-dynamics. In the following sections, two different cascaded control approaches are discussed.

A. Incremental Control Approach

1) Outer-Loop Position Control: The outer-loop command of the incremental approach is computed using NDI by utilizing the dynamics of piston and external-load. The area of chamber B is A_B, which can be related to that of chamber A as A_A=A_B+A_r, where A_r refers to the piston-area. Using this relation in Eq. (1), the following equation is obtained:

$$(M_L + M_p)\,\ddot{x} + F_f + F_L = (P_A - P_B)A_A + P_B A_r - P_a A_r \tag{6}$$

Before proceeding to model inversion, the friction force F_f is ignored, as they can be oscillatory for some part of the trajectory, which will then be reflected in the final NDI output. It should be noted that even though F_f is ignored in the controller design, but it is included while simulating the plant dynamics. The designed NDI controller thus involves a partial dynamic inversion [19]. Next, by introducing the linear control law $\ddot{x} = v_1$ in Eq. (6), the expression for desired pressure-difference across the chambers is calculated as follows:

$$P_{L_d} = \frac{(M_p + M_L)\,v_1 + P_a A_r - P_B A_r + F_l}{A_A} \tag{7}$$

In Eq. (7), it is assumed that the external load F_l is known and measured using a force sensor. P_{L_d} refers to the difference of pressure between the two chambers of cylinder. The linear control law v_1 is chosen as follows:

$$\begin{aligned} v_1 =& K_{p_1}\,(x_d(t) - x(t)) + K_{d_1}(\dot{x}_d(t) - \dot{x}(t)) \\ &+ K_{i_1} \sum \left((x_d(t) - x(t))\,\Delta t\right) \end{aligned} \tag{8}$$

In Eq. (8), x_d refers to the desired piston-position, x is the actual piston-position and the tuning parameters are denoted by K_{p_1}, K_{d_1} and K_{i_1}. Δt is the sampling time of the simulation.

2) Inner-Loop Force Control: The inner-loop control is based on INDI and is also known as a force control loop [18]. In order to derive the INDI control law, the mass-flow rate in Eq. (4) is equated in Eq. (2). Furthermore, by utilizing the expression for the differential pressure P_L, the equation of motion can be as expressed as $\dot{P}_L = f(A_v, \text{Other Parameters})$, where f refers to a function that depends on the orifice-opening A_v and other parameters, which includes the flow-rate constants C_f, C_1 and C_2, the ideal-gas constant R, the temperature T, the specific heat-ratio k, the complete stroke-length L, the inactive chamber-volume V_0, the area of chambers A_A and A_B, and the position of the piston x. Next, similar to Section III, by utilizing a high-sampling rate of the system, the relation $\dot{P}_L = \dot{P}_{L_0} + G(A_v - A_{v_0})$ is obtained, where $\dot{P}_{L_0}$ refers to the derivative of actual pressure-difference across the chambers at the previous sampling-instant. A_v and A_{v_0} denote the orifice opening of the valve, measured at the current and previous time-instant, respectively.

As mentioned in Section III, INDI is robust to variations in the control-effectiveness G that is introduced previously in Eq. (5). Therefore, a fixed control-effectiveness of magnitude $3 \cdot 10^8\ Pa \cdot s^{-1} \cdot m^{-2}$ is used here, which is chosen after carefully analyzing the time-domain response of the INDI-controlled system, and then averaging the value of G over the whole simulation period. Next, by introducing the linear control law $\dot{P}_L$ = v_2 and by using inversion similar to Eq. 5, the relation $A_v = A_{v_0} + G^{-1}\left(v_2 - \dot{P}_{L_0}\right)$ is obtained for the final INDI control-output. The linear control-law v_2 is summarized below in Eq. (9), where K_{p_2} and K_{i_2} are the tuning parameters.

$$v_2 = \dot{P}_{L_d}(t) + K_{p_2}\left(P_{L_d}(t) - P_L(t)\right) + K_{i_2} \sum \left(\left(P_{L_d}(t) - P_L(t)\right)\Delta t\right) \tag{9}$$

B. PID Control Approach

1) Outer-Loop Position Control: It is summarized in Eq. (10), where K_{p_3}, K_{d_3} and K_{i_3} denotes the proportional, derivative and integral constants of the PID, respectively.

$$\begin{aligned} P_{L_d} =& K_{p_3}\,(x_d(t) - x(t)) + K_{d_3}(\dot{x}_d(t) - \dot{x}(t)) \\ &+ K_{i_3} \sum \left((x_d(t) - x(t))\,\Delta t\right) \end{aligned} \tag{10}$$

2) Inner-Loop Force Control: It is summarized in Eq. (11), where K_{p_4}, K_{d_4} and K_{i_4} are the tuning parameters.

$$\begin{aligned} A_v =& K_{d_4}(\dot{P}_{L_d}(t) - \dot{P}_L(t)) + K_{p_4}\,(P_{L_d}(t) - P_L(t)) \\ &+ K_{i_4} \sum \left(\left(P_{L_d}(t) - P_L(t)\right)\Delta t\right) \end{aligned} \tag{11}$$

In Eqs. (8), (9), (10) and (11), the terms proportional to the velocity and position error are sufficient for obtaining the desired time-domain characteristics such as rise-time and overshoot. However to ensure a zero steady-state error between the reference and the actual trajectory of the cylinder-piston, the integral term is added.

V. Simulation Results

The tracking results of the incremental control approach is compared with that of a PID in three different conditions. Error measures such as root mean square error (RMSE) and absolute error are used for the comparison of the incremental approach with the baseline PID controller. Prior to these comparisons, both the controllers are tuned to achieve similar time-domain characteristics such as rise-time, settling-time and overshoot. The controllers are tuned using a step response such that there is no overshoot in their response. Moreover, a difference of 0.08 seconds is observed in the rise-time of outer-loop response of the two controllers. For the inner-loop responses, a difference of 0.6 seconds is observed in the settling-time of the two approaches, which is acceptable for our application. The sampling time for the simulations was 0.1 milliseconds.

A. Controller Comparison under Nominal Conditions

The controller is initially analyzed under nominal conditions where sensor noises are not added and the external-load is considered as 2,000 N. The amplitude and frequency of this reference sinusoidal signal are chosen as 0.5 m and 0.2356 rad/s, respectively. The dimensions of the pneumatic system are summarized in Table. I.

TABLE I: Dimensions of a long-stroke pneumatic system

Parameter	Long-stroke pneumatic system
Piston stroke (L)	1.2 m
Equivalent Length of dead volume (L_0)	0.1 m
Chamber diameter (d_c)	0.16 m
Rod diameter (d_p)	0.032 m
External load mass (M_L)	200 kg
Piston plus rod mass (M_p)	2 kg
Maximum orifice opening ($A_{v_{\max}}$)	$2.2062 \cdot 10^{-3}$ m^2
Maximum supply pressure (P_s)	10 bar

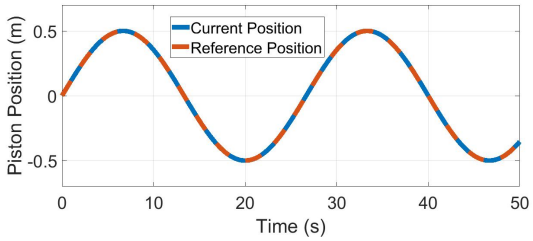

(a) Nominal case tracking results of incremental approach

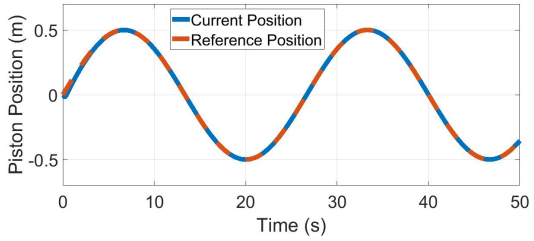

(b) Nominal case tracking results of PID

Fig. 3: Tracking results for a nominal case of external load F_L=2,000 N

The tracking results and the tracking errors for the nominal-case are plotted in Fig. 3 and Fig. 4, respectively. The tracking errors are calculated only after the control inputs stabilize, i.e., all the simulation transients have died out. Besides this, some extra margin is considered and thus a time range of 10-50 seconds is used for calculating the errors of both the controllers. It is observed that for both the outer-loop position controllers, all the three error measures are minimal. For instance, the RMSE of outer loop PID is 0.62 mm, whereas the RMSE of outer-loop incremental approach is 0.14 mm. For the inner-loop, tracking errors of PID are higher than that of its incremental counterpart. For instance, the RMSE error of PID is 64.7% higher than its incremental counterpart. We also observe that for the inner-loop tracking error of incremental approach, peaks are observed at 20, 33 and 47 seconds. The reason for this observation is that these points mark the turn-around points of the reference

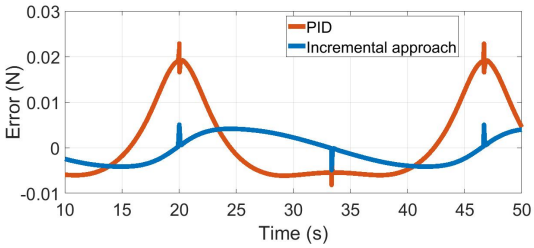

(a) Inner-loop tracking errors of PID and incremental approach

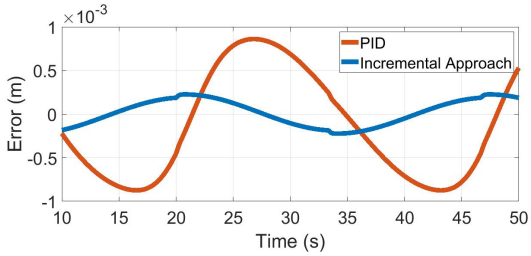

(b) Outer-loop tracking errors of PID and incremental approach

Fig. 4: Tracking errors of incremental control approach and PID for a nominal case of external load F_L=2,000 N

trajectory to be tracked, where the rate of change of chamber-pressure changes its direction. This further causes a jump in the calculated pressure-derivative due to this discontinuity, which is then reflected in the output of incremental approach and finally in the inner-loop error.

B. Controller Comparison under Varying External Load

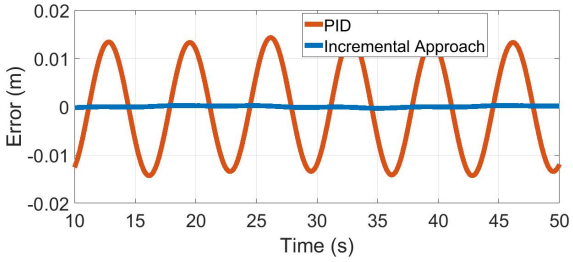

Fig. 5: Nominal-case tracking errors of PID and incremental approach for varying load

The nominal mass of the external load is considered to be 200 kg and the value of gravitational constant g is taken as 9.8 m/s^2. The variation of the gravitational component felt by the cylinder is done by considering a sinusoidal motion about a base point that is fixed to the ground. The axis of rotation is directly perpendicular to the axis of motion of the cylinder which will ensure a two-dimensional motion of the cylinder, besides ensuring that the component of gravity acting directly along the axis of cylinder will keep changing throughout the tracking trajectory. The outer-loop tracking RMSE of incremental approach is 98.4% lower than that of the PID (Fig. 5). The reason for such a disparity in the tracking errors is because the incremental approach considers the varying load in its controller formulation, as is expressed

using Eq. (7). However, the output of corresponding PID control does not directly depend on the varying load, but rather only on the piston-position error and its time-derivative, as expressed in Eq. (10).

C. Controller Comparison in the Presence of Sensor Noise

In order to test the robustness property of both the control approaches, normally distributed Gaussian noise is introduced in both the simulated piston-position and the chamber-pressure sensors. The accuracy of both the position and chamber-pressure feedback is found after a survey of a few available sensors [20], [21]. The feedback of piston-velocity and the chamber pressure-derivative are obtained using numerical-differentiation of their parent variable. The properties of the simulated sensor noise are summarized in the Table. II. In order to attenuate the sensor noise, a first

TABLE II: Summary of simulated sensor noise

Sensor	Piston-Position	Chamber-Pressure
Mean error	$-9{\cdot}10^{-9}$ m	0.09 Pa
Maximum error	$1.1 \cdot 10^{-4}$ m	1,114.3 Pa
Standard-deviation of error	$2.49 \cdot 10^{-5}$ m	249.8 Pa

order filter is implemented. Two sets of filtering schemes are tested named as moderate-filtering and high-filtering. The cut-off frequencies of high-filtering scheme is set to be lower than the moderate-filtering scheme. A filter with a lower cut-off frequency than the system's cut-off frequency will ensure that besides noise, some useful information from the plant dynamics is also filtered out. Thus, these two schemes involve a trade-off between useful information content and sensor noise, which will be used for comparing the two control schemes.

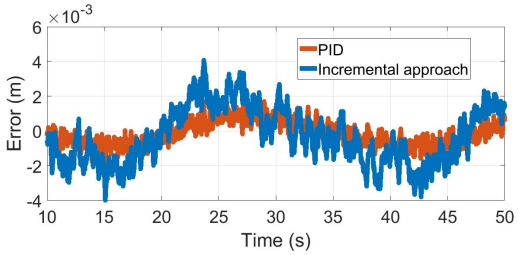

(a) Robust case outer-loop tracking errors without filtering

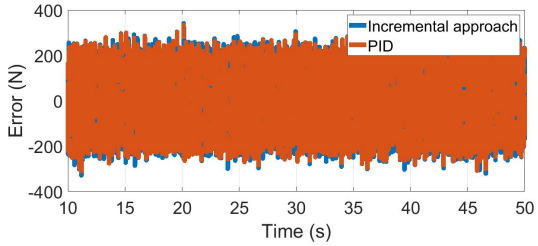

(b) Robust case inner-loop tracking errors without filtering

Fig. 6: Robust case tracking errors without filtering

It is observed from Figs. 6, 7 and 8 that the errors significantly reduced after the introduction of low-pass filters. For

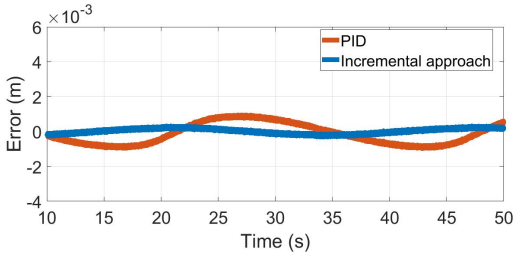

(a) Robust case outer-loop tracking errors with moderate filtering

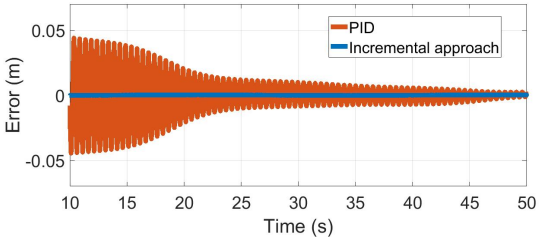

(b) Robust case outer-loop tracking errors with high filtering

Fig. 7: Robust case outer-loop tracking errors with filtering

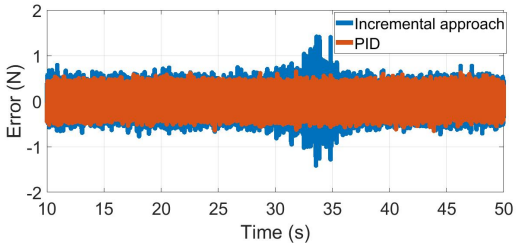

(a) Robust case inner-loop tracking errors with moderate filtering

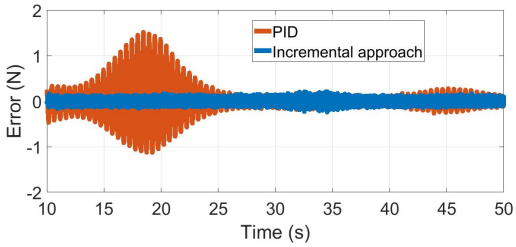

(b) Robust case inner-loop tracking errors with high filtering

Fig. 8: Robust case inner-loop tracking errors with filtering

instance, the outer-loop mean absolute tracking error reduced by over 10 times, as compared to the corresponding unfiltered scenario of the incremental approach. It is also found that the RMSE of outer-loop incremental approach is lower than the outer-loop PID by 75.84% but however, the RMSE of inner-loop incremental approach is higher than inner-loop PID by 26.3% for the moderate filtering scheme. The absolute error of inner-loop PID is lower than inner-loop incremental approach by 26.6% and this trend is also found in their corresponding RMSE. Therefore it can be concluded from these observations that in the presence of moderate filtering scheme, the inner-loop and outer-loop errors do not show a similar trend for both the control approaches. Following this, the introduction of high-filtering further reduced the

inner-loop tracking errors for the incremental approach by around 83.0% as compared to its corresponding error using moderate filtering. However, with the high-filtering scheme, PID showed degradation, with the error rising by 57.0% as compared to the corresponding moderate filtering results. It can also be observed that the RMSE of the inner-loop incremental approach is 87.7% lower than that of the inner-loop PID. A similar trend is also found in the outer-loop, where the RMSE of PID is greater than the incremental approach by 98.9%. Therefore, it can be concluded from these results that if the cut-off frequency of filter is increased to attenuate more noise, similar to our high-filtering scheme, then the incremental approach will perform better than PID. However, in the absence of any filters or with the moderate-filtering scheme, no clear advantage of a particular control approach was found.

VI. CONCLUSIONS AND FUTURE WORK

A cascaded-control strategy based on incremental nonlinear dynamic inversion control is successfully designed in this paper, for position-tracking tasks using a long-stroke pneumatic cylinder. The performance of the incremental control approach is compared with a PID, and it is found to be similar and satisfactory for the nominal case, with the maximum absolute error being less than 1% of the reference amplitude for both the controllers.

Furthermore, realistic sensor noises are introduced in the system, which are then filtered using two different filtering schemes as a result of which the performance of both the control approaches increased, when compared with the unfiltered approach. For the incremental control approach, there is a significant decrease of over 99% in the RMSE of the inner-loop tracking using the high filtering incremental approach. However, this is not the case with the response obtained from PID, thus glorifying the robustness of incremental control approach in the presence of realistic sensor noise, by utilizing comparatively less information of plant dynamics. It is also found that for the case of varying external load, the RMSE of outer-loop tracking error of the incremental approach is around 98% higher than for the PID. Therefore, it can be concluded that incremental control approach has potential in increasing the tracking performance of pneumatic actuators, as observed from a number of simulation scenarios in this research article.

The outer-loop of the incremental approach that is currently based on NDI can be designed using INDI in future research, which will further reduce the dependency of the controller on the system states. The compressibility effects of the pneumatic cylinder also needs to be studied in more detail in order to find its dependency on the chamber volumes. Moreover, the variation of the cut-off frequency of the low-pass filters require more investigation in order to find the maximum efficiency of the incremental controller in the presence of sensor noises. Besides this, more study is required for finding the instability in the designed controlled system due to low-pass filtering.

REFERENCES

[1] H. I. Ali, S. Noor, S. Bashi, and M. Marhaban, "A review of pneumatic actuators (modeling and control)," *Australian Journal of Basic and Applied Sciences*, vol. 3, no. 2, pp. 440–454, 2009.

[2] Y. Huang, "Incremental nonlinear control of hydraulic parallel robots: An application to the simona research simulator," Ph.D. dissertation, Delft University of Technology, 2019.

[3] L. An and N. Sepehri, "Hydraulic actuator leakage fault detection using extended kalman filter," *International Journal of Fluid Power*, vol. 6, no. 1, pp. 41–51, 2005.

[4] P. Szczepaniak, G. Jastrzebski, and M. Jóźko, "A method of investigating internal leakages in aircraft hydraulic units," *Journal of KONES*, vol. 21, 2014.

[5] S. Liu and J. Bobrow, "An analysis of a pneumatic servo system and its application to a computer-controlled robot," *Journal of dynamic systems, measurement, and control*, vol. 110, no. 3, pp. 228–235, 1988.

[6] J. E. Bobrow and F. Jabbari, "Adaptive pneumatic force actuation and position control," in *1989 American Control Conference*. IEEE, 1989, pp. 1508–1513.

[7] M. Trumić, K. Jovanović, and A. Fagiolini, "Decoupled nonlinear adaptive control of position and stiffness for pneumatic soft robots," *The International Journal of Robotics Research*, p. 0278364920903787, 2020.

[8] Z. Rao and G. M. Bone, "Modeling and control of a miniature servo pneumatic actuator," in *Proceedings 2006 IEEE International Conference on Robotics and Automation, 2006. ICRA 2006.* IEEE, 2006, pp. 1806–1811.

[9] H.-P. Ren, X. Wang, J.-T. Fan, and O. Kaynak, "Fractional order sliding mode control of a pneumatic position servo system," *Journal of the Franklin Institute*, 2019.

[10] S. Jacklin, J. Schumann, P. Gupta, M. Lowry, J. Bosworth, E. Zavala, K. Hayhurst, C. Belcastro, and C. Belcastro, "Verification, validation, and certification challenges for adaptive flight-critical control system software," in *AIAA Guidance, Navigation, and Control Conference and Exhibit*, 2004, p. 5258.

[11] S. Sieberling, Q. Chu, and J. Mulder, "Robust flight control using incremental nonlinear dynamic inversion and angular acceleration prediction," *Journal of guidance, control, and dynamics*, vol. 33, no. 6, pp. 1732–1742, 2010.

[12] P. Simplício, M. Pavel, E. Van Kampen, and Q. Chu, "An acceleration measurements-based approach for helicopter nonlinear flight control using incremental nonlinear dynamic inversion," *Control Engineering Practice*, vol. 21, no. 8, pp. 1065–1077, 2013.

[13] H. Das, "Dynamic inversion control of quadrotor with a suspended load," *IFAC-PapersOnLine*, vol. 51, no. 1, pp. 172–177, 2018.

[14] M. Malaysia, "Non-linear modeling and cascade control of an industrial pneumatic actuator system," *Australian Journal of Basic and Applied Sciences*, vol. 5, no. 8, pp. 465–477, 2011.

[15] E. Richer and Y. Hurmuzlu, "A high performance pneumatic force actuator system: Part i—nonlinear mathematical model," *J. dyn. sys., meas., control*, vol. 122, no. 3, pp. 416–425, 1999.

[16] H. Das, K. Sridhar, and R. Padhi, "Bio-inspired landing of quadrotor using improved state estimation," *IFAC-PapersOnLine*, vol. 51, no. 1, pp. 462–467, 2018.

[17] X. Wang, E.-J. Van Kampen, Q. Chu, and P. Lu, "Stability analysis for incremental nonlinear dynamic inversion control," *Journal of Guidance, Control, and Dynamics*, vol. 42, no. 5, pp. 1116–1129, 2019.

[18] Y. Huang, D. M. Pool, O. Stroosma, and Q. Chu, "Long-stroke hydraulic robot motion control with incremental nonlinear dynamic inversion," *IEEE/ASME Transactions on Mechatronics*, vol. 24, no. 1, pp. 304–314, 2019.

[19] S. S. Mulgund and R. F. Stengel, "Aircraft flight control in wind shear using partial dynamic inversion," in *1993 American Control Conference*. IEEE, 1993, pp. 400–404.

[20] I. L. Krivts and G. V. Krejnin, *Pneumatic actuating systems for automatic equipment: structure and design*. Crc Press, 2016.

[21] P. Rohner, *Fluid Power Logic Circuit Design: Analysis, Design Methods and Worked Examples*. Macmillan International Higher Education, 1979.